Performance Improvement of Joint THP/pre-FDE With Lattice Reduction Using LLL-algorithm

Kazuki TAKEDA† Hiromichi TOMEBA† and Fumiyuki ADACHI‡

Dept. of Electrical and Communications Engineering, Graduate School of Engineering, Tohoku University
6-6-05 Aza-Aoba, Aramaki, Sendai, 980-8579 Japan

†{kazuki, tomeba}@mobile.ecei.tohoku.ac.jp ‡adachi@ecei.tohoku.ac.jp

***Abstract*— Average bit error rate (BER) performance of single-carrier (SC) transmission significantly degrades due to the strong inter-symbol interference (ISI) in a severe frequency-selective fading channel. Recently, we proposed a joint Tomlinson-Harashima precoding (THP)/frequency-domain pre-equalization (pre-FDE) using LQ-decomposition to improve the BER performance of SC transmission. However, since the dummy symbols insertion is necessary, the data rate reduces. In this paper, we apply LLL-algorithm to joint THP/pre-FDE to avoid the dummy symbol insertion and evaluate the BER performance by computer simulation.**

Keywords-components; Pre-equalization, Tomlinson-Harashima precoding, LLL-algorithm

I. INTRODUCTION

In the next generation mobile communication systems, broadband data transmission services are demanded [1]. Since the broadband wireless channel is composed of many distinct propagation paths having different time delays, the single-carrier (SC) transmission performance significantly degrades due to inter-symbol interference (ISI) arising from severe frequency-selective channel [2]. Frequency-domain equalization (FDE) based on the minimum mean square error (MMSE) criterion can improve the bit error rate (BER) performance [3-4]. However, the residual ISI after FDE limits the performance improvement [5]. The performance gap from the theoretical lower bound gets larger as higher-level quadrature amplitude modulation (QAM) is used.

Recently, we proposed a joint use of Tomlinson-Harashima precoding (THP) [6-7] at a transmitter and FDE at a receiver (called joint THP/FDE) for SC transmission [8-9]. We showed by numerical analysis and computer simulation that the joint THP/FDE significantly improves the BER performance of SC transmission compared to the case of using MMSE-FDE at a receiver. However, joint THP/FDE requires the channel state information and computationally expensive signal processing at both the transmitter and receiver. A simpler mobile terminal is desirable. We proposed joint THP/frequency-domain pre-equalization (pre-FDE) (joint THP/pre-FDE) [10] for downlink data transmission. Since pre-FDE is carried out at the transmitter, joint THP/pre-FDE can alleviate the complexity problem of mobile terminals and suitable for downlink applications. We demonstrated by computer simulation that joint THP/pre-FDE can provide almost the same BER performance as joint THP/FDE.

Assuming perfect CSI, joint THP/pre-FDE can perfectly cancel the residual ISI while achieving the frequency-diversity gain. This is because the equivalent channel (the concatenation of the pre-FDE circulant filter and the propagation channel) is transformed into a causal channel by the use of LQ-decomposition [11] so that THP can remove the residual ISI. The received signal power depends on the diagonal elements of a lower triangular matrix **B**, obtained by LQ-decomposition of the equivalent channel matrix. As shown in [10], since the equivalent channel matrix is represented by a circulant matrix, the amplitude of the diagonal element of **B** closer to lower right position drops. This degrades the BER performance achievable with joint THP/pre-FDE. To avoid this performance degradation, the dummy symbols insertion is necessary at the end of the signal block. However, this dummy symbol insertion reduces the transmission rate.

To avoid the dummy symbol insertion, a lattice reduction using LLL-algorithm [12-13] can be used. In Refs. [14-15], the LLL-algorithm is used to improve the BER performance of multi-input multi-output (MIMO) multiplexing with successive interference cancellation (SIC). In this paper, we apply the LLL-algorithm to joint THP/pre-FDE to mitigate the amplitude drop of the diagonal elements of **B** and hence to avoid the dummy symbol insertion. We show by computer simulation that the application of LLL-algorithm can improve the BER performance.

The remainder of this paper is organized as follows. Sect. II points out the problem of previously proposed joint THP/pre-FDE. In Sect. III, we apply the LLL-algorithm to joint THP/pre-FDE. Sect. IV discusses the computer simulation results. Sect. V concludes this paper.

II. PROBLEM OF JOINT THP/PRE-FDE

A. Overall transmission system model

The overall transmission system model of previously proposed joint THP/pre-FDE is illustrated in Fig. 1. In this paper, symbol-spaced discrete time signal representation is used. The transmit signal vector $\mathbf{s}=[s(0), \ldots, s(t), \ldots, s(N_c-1)]^T$ represents the data modulated symbol block. At the transmitter, THP is applied to **s** to obtain the signal vector $\mathbf{x}=[x(0), \ldots, x(t), \ldots, x(N_c-1)]^T$. Then, an $(N_c \times N_c)$ matrix $C \cdot \mathbf{Q}^H \{diag(\mathbf{Q})\}^{-1}$, which will introduced later in Eq. (10), is multiplied to **x**. The resultant signal vector $\mathbf{y}=[y(0), \ldots, y(t), \ldots, y(N_c-1)]^T$ is input to the pre-FDE block in Fig. 1. Then, after the insertion of cyclic prefix (CP) into the guard interval (GI), the pre-FDE

output signal is transmitted over a frequency-selective channel. The channel gain $H(k)$ at the kth frequency is given by

$$H(k)=\sum_{l=0}^{L-1} h_l \exp\left(-j2\pi k\frac{\tau_l}{N_c}\right), \quad (1)$$

where h_l and τ_l represent the complex valued path gain with $\sum_{l=0}^{L-1} E[|h_l|^2]=1$ and the delay time of the lth path, respectively.

At the receiver, after the removal of GI, the modulo operation [16] is applied to the received signal to obtain the soft decision symbol vector $\hat{\mathbf{s}}$ =[$\hat{s}(0)$, …, $\hat{s}(t)$, …, $\hat{s}(N_c-1)$]^T.

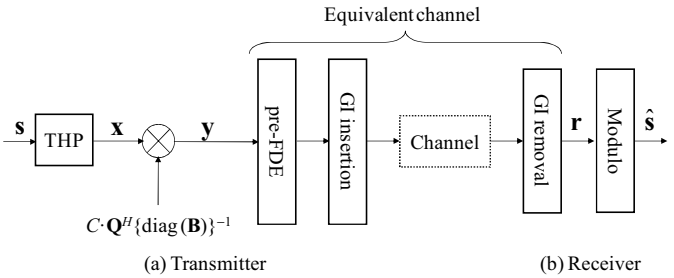

Fig. 1 Overall transmission system model with previously proposed joint THP/pre-FDE.

B. pre-FDE

In pre-FDE, the signal vector $\mathbf{y}$ is transformed by using N_c-point fast Fourier transform (FFT) into the frequency-domain transmit signal, to which the FDE weights are multiplied. The frequency-domain transmit signal after pre-FDE is transformed by using N_c-point inverse FFT (IFFT) back into the time-domain signal and is transmitted after the GI insertion. The received signal $\{r(t);\ t=0\sim N_c-1\}$ can be expressed using the vector form as

$$\mathbf{r}=[r(0),\ \cdots,\ r(t),\ \cdots,\ r(N_c-1)]^T=\sqrt{\frac{2E_s}{T_s}}\hat{\mathbf{h}}\mathbf{y}+\mathbf{n}, \quad (2)$$

where E_s is the average transmit symbol energy. $\mathbf{n}$=[$n(0)$, …, $n(t)$, …, $n(N_c-1)$]^T is the noise vector, whose elements are the independent and identically distributed Gaussian variables with zero-mean and variance $2N_0/T_s$, where N_0 is the one-sided additive white Gaussian noise (AWGN) power spectrum density. In this paper, a concatenation of pre-FDE and the propagation channel is called the equivalent channel. $\hat{\mathbf{h}}$ in Eq. (2) is the equivalent channel matrix of size ($N_c\times N_c$), given by

$$\hat{\mathbf{h}}=\begin{bmatrix} \hat{h}_0 & \hat{h}_{N_c-1} & \ddots & \hat{h}_1 \\ \hat{h}_1 & \hat{h}_0 & \ddots & \vdots \\ \vdots & \hat{h}_1 & \ddots & \hat{h}_{N_c-1} \\ \hat{h}_{N_c-1} & \vdots & \ddots & \hat{h}_0 \end{bmatrix}, \quad (3)$$

where $\hat{h}_l$, l=0~N_c–1, is the impulse response of the equivalent channel with

$$\hat{h}_l=\frac{1}{N_c}\sum_{k=0}^{N_c-1} w(k)H(k)\exp\left(j2\pi k\frac{l}{N_c}\right). \quad (4)$$

In the above, $w(k)$ is the pre-FDE weight.

There are four well-known FDE weights based on the zero-forcing (ZF), equal gain combining (EGC), maximum ratio combining (MRC), and MMSE criterion. It was found by computer simulation in [9] that the pre-FDE weight using (EGC) provide the best BER performance. In this paper, we use the pre-FDE using EGC weight given by

$$w(k)=H(k)/|H(k)|. \quad (5)$$

It can be understood from Eqs. (2) and (3) that the residual ISI is produced due to the presence of the non-diagonal elements in $\hat{\mathbf{h}}$. To remove the residual ISI, THP is introduced.

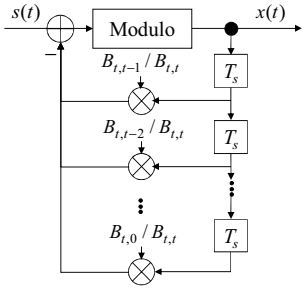

Fig. 2 THP structure.

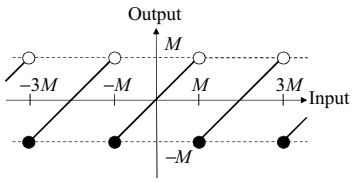

Fig. 3 Modulo operator.

C. THP

THP structure is illustrated in Fig. 2. $B_{i,j}$ is the (i, j)th element of a lower triangular matrix $\mathbf{B}$ obtained by the LQ-decomposition of $\hat{\mathbf{h}}$ as

$$\hat{\mathbf{h}}=\mathbf{BQ}=\begin{bmatrix} B_{0,0} & & \mathbf{0} \\ \vdots & \ddots & \\ B_{N_c-1,0} & \cdots & B_{N_c-1,N_c-1} \end{bmatrix}\mathbf{Q}, \quad (6)$$

where $\mathbf{Q}$ is the orthogonal unitary matrix.

The THP removes the residual ISI caused by the non-diagonal elements in $\hat{\mathbf{h}}$. The THP employs a modulo operator to keep the transmit signal amplitude within a certain value. The real and imaginary parts of the modulo operator output are limited in the range of [–M, M), where M is the real-valued modulo operation size (see Fig. 3). $\mathbf{x}$ can be written as

$$\mathbf{x}=\mathbf{s}-(\mathbf{B}-diag(\mathbf{B}))\{diag(\mathbf{B})\}^{-1}\mathbf{x}+2M\mathbf{z}_t. \quad (7)$$

This can be further simplified as

$$\mathbf{x}=\{diag(\mathbf{B})\}\mathbf{B}^{-1}(\mathbf{s}+2M\mathbf{z}_t), \quad (8)$$

where $diag(\mathbf{B})$ denotes the diagonal matrix whose diagonal elements are equal to those of $\mathbf{B}$. $2M\mathbf{z}_t$=[$2Mz_t(0)$, …, $2Mz_t(t)$,

…, $2Mz_t(N_c-1)]^T$ represents the modulo operation in THP. The real and imaginary parts of all the elements of $\mathbf{z}_t$ are an integer.

After applying THP, the THP output vector is multiplied by $C\cdot\mathbf{Q}^H\{diag(\mathbf{B})\}^{-1}$ to obtain the pre-FDE input signal vector $\mathbf{y}$ as

$$\mathbf{y} = C\cdot\mathbf{Q}^H\{diag(\mathbf{B})\}^{-1}\mathbf{x} = C\cdot\mathbf{Q}^H\mathbf{B}^{-1}(\mathbf{s}+2M\mathbf{z}_t), \quad (9)$$

where C is the power normalization coefficient to keep the average transmit signal power intact and is given by

$$C = \sqrt{N_c / \sum_{\tau=0}^{N_c-1}(1/|B_{\tau,\tau}|^2)}. \quad (10)$$

Then, pre-FDE is carried out on $\mathbf{y}$ as described in Sec. II B.

Substituting Eqs. (6) and (9) into Eq. (2), the received signal vector $\mathbf{r}$ can be rewritten as

$$\mathbf{r} = \sqrt{\frac{2E_s}{T_s}}C\cdot(\mathbf{s}+2M\mathbf{z}_t)+\mathbf{n}, \quad (11)$$

which indicates that joint THP/pre-FDE perfectly remove the residual ISI (if the perfect CSI is assumed).

D. Problem

LQ-decomposition can be implemented by the use of Gram-Schmidt orthogonalization method [11]. Let the ith column vectors of $\hat{\mathbf{h}}$ and $\mathbf{Q}$ be denoted by $\hat{\mathbf{h}}_i$ and $\mathbf{Q}_i$, respectively. The (i, j)th element $B_{i,j}$ of $\mathbf{B}$ is given as

$$\begin{cases} B_{i,i} = \left\| \hat{\mathbf{h}}_i - \sum_{j=0}^{i-1}(\mathbf{Q}_j^H\hat{\mathbf{h}}_i)\mathbf{Q}_j \right\|, & i = j \\ B_{i,j} = (\mathbf{Q}_j^H\hat{\mathbf{h}}_i), & i \neq j \end{cases}, \quad (12)$$

where

$$\mathbf{Q}_i = \frac{1}{B_{i,i}}\left\{\hat{\mathbf{h}}_i - \sum_{j=0}^{i-1}(\mathbf{Q}_j^H\hat{\mathbf{h}}_i)\mathbf{Q}_j\right\} \quad (13)$$

is a linear combination of $\{\hat{\mathbf{h}}_j ; j=0\sim i-1\}$. $|B_{i,i}|$ strongly depends on the correlation between $\hat{\mathbf{h}}_i$ and $\{\hat{\mathbf{h}}_j ; j=0\sim i-1\}$. The circulant property of $\hat{\mathbf{h}}$ results in the large cross-correlation between $\{\hat{\mathbf{h}}_i ; i=0, 1, \ldots\}$ near the leftmost position and $\{\hat{\mathbf{h}}_j ; j=\ldots, N_c-2, N_c-1\}$ near the rightmost position. Therefore, some $|B_{i,i}|$'s at the position near the right side of $\mathbf{B}$ have small values. If $|B_{\tau,\tau}|\rightarrow 0$ at a certain τ, we have $C\rightarrow 0$ and the received signal power drops.

To avoid the amplitude drop of the diagonal elements near the lower right side of $\mathbf{B}$, we apply LLL-algorithm.

III. Application of LLL-algorithm to Joint THP/pre-FDE

A. LLL-algorithm

The LLL-algorithm [12] transforms the matrix $\hat{\mathbf{h}}$ into a new matrix $\hat{\mathbf{h}}^L$. $\hat{\mathbf{h}}^L$ is written as

$$\hat{\mathbf{h}}^L = \mathbf{B}^L\mathbf{Q}^L, \quad (14)$$

where $\mathbf{B}^L$ and $\mathbf{Q}^L$ are an lower triangular matrix and an orthogonal unitary matrix obtained by the LQ-decomposition of $\hat{\mathbf{h}}^L$. The (k, l)th element of $\mathbf{B}^L$ satisfies

$$|B_{k,l}^L| \le \frac{1}{2}|B_{l,l}^L|, \quad 0 \le l < k < N_c - 1 \quad (15)$$

and

$$\delta|B_{k,k}^L|^2 \le |B_{k+1,k+1}^L|^2 + |B_{k+1,k}^L|^2 \text{ with } \frac{1}{4} < \delta \le 1. \quad (16)$$

From Eqs. (15) and (16), the diagonal elements of $\mathbf{B}^L$ have larger absolute values than those of $\mathbf{B}$ obtained by LQ-decomposition of $\hat{\mathbf{h}}$. δ is a parameter.

The LLL-algorithm keeps the lattice of the original matrix intact even after the matrix transformation. $\hat{\mathbf{h}}^L$ can be rewritten using $\hat{\mathbf{h}}$ (=$\mathbf{BQ}$ in Eq. (7)) as

$$\hat{\mathbf{h}}^L = \mathbf{B}^L\mathbf{Q}^L = \mathbf{TBQ} = \mathbf{T}\hat{\mathbf{h}}, \quad (17)$$

where $\mathbf{T}$ is an $(N_c\times N_c)$ matrix having the property of

$$\{\mathrm{Re}[T_{i,j}], \mathrm{Im}[T_{i,j}]\} \in \mathbf{Z}, \quad |\det(\mathbf{T})| = 1 \quad \text{for } 0 \le i, j < N_c, \quad (18)$$

where $\mathbf{Z}$ denotes the set of all integers.

B. Joint THP/pre-FDE using LLL-algorithm

Figure 4 illustrates the overall transmission system model of joint THP/pre-FDE using LLL-algorithm. The difference between the conventional joint THP/pre-FDE shown in Fig. 1 and the proposed joint THP/pre-FDE using LLL-algorithm is the introduction of multiplication of the $(N_c\times N_c)$ matrix $\mathbf{T}$.

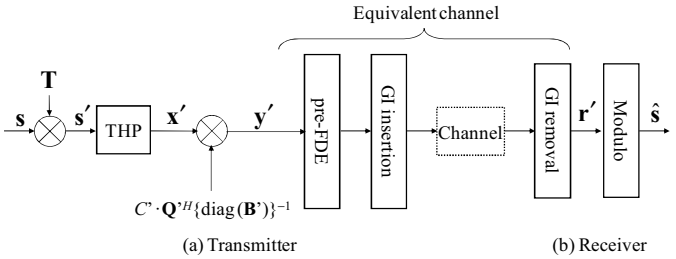

Fig. 4 Overall transmission system model with proposed joint THP/pre-FDE using LLL-algorithm.

At first, $\mathbf{T}$ is multiplied to the data symbol vector $\mathbf{s}$ as

$$\mathbf{s}' = \mathbf{Ts}. \quad (19)$$

Next, THP is carried out. The THP output signal vector $\mathbf{x}'=[x'(0), \ldots, x'(t), \ldots, x'(N_c-1)]^T$ is expressed as

$$\mathbf{x}' = \mathbf{s}' - (\mathbf{B}^L - diag(\mathbf{B}^L))\{diag(\mathbf{B}^L)\}^{-1}\mathbf{x}' + 2M\mathbf{z}_t, \quad (20)$$

which can be further simplified, similar to Eq. (9), as

$$\mathbf{x}' = \{diag(\mathbf{B}^L)\}(\mathbf{B}^L)^{-1}(\mathbf{s}' + 2M\mathbf{z}_t). \quad (21)$$

The THP output signal vector $\mathbf{x}'$ is multiplied by $C'\cdot(\mathbf{Q}^L)^H\{diag(\mathbf{B}^L)\}^{-1}$. From Eq. (21), the resultant signal vector $\mathbf{y}'=[y'(0), \ldots, y'(t), \ldots, y'(N_c-1)]^T$ is given as

$$\begin{aligned}\mathbf{y}' &= C' \cdot (\mathbf{Q}^L)^H \{diag(\mathbf{B}^L)\}^{-1} \mathbf{x}' \\ &= C' \cdot (\mathbf{Q}^L)^H (\mathbf{B}^L)^{-1} (\mathbf{s}' + 2M\mathbf{z}_t)\end{aligned}, \quad (22)$$

where $C' = \sqrt{N_c / \sum_{\tau=0}^{N_c-1} (1/|B^L_{\tau,\tau}|^2)}$ is the power normalization coefficient. Then, $\mathbf{y}'$ is input to the pre-FDE block in Fig. 4. After the insertion of cyclic prefix into the GI, the pre-FDE output signal is transmitted.

Similar to Eq. (2), the received signal vector $\mathbf{r}'=[r'(0), \ldots, r'(t), \ldots, r'(N_c-1)]^T$ can be expressed using $\hat{\mathbf{h}}$ and the pre-FDE input signal vector $\mathbf{y}'$ as

$$\mathbf{r}' = \sqrt{\frac{2E_s}{T_s}} \hat{\mathbf{h}} \mathbf{y}' + \mathbf{n}. \quad (23)$$

Substituting Eqs. (17) and (22) into Eq. (23) gives

$$\mathbf{r}' = \sqrt{\frac{2E_s}{T_s}} C' \cdot (\mathbf{s} + \mathbf{T}^{-1} 2M\mathbf{z}_t) + \mathbf{n}, \quad (24)$$

Note that the real and imaginary parts of each element of $\mathbf{T}^{-1}$ are an integer and $|\det(\mathbf{T}^{-1})|=1$. Therefore, Eq. (24) can be rewritten as

$$\mathbf{r}' = \sqrt{\frac{2E_s}{T_s}} C' \cdot (\mathbf{s} + 2M\tilde{\mathbf{z}}_t) + \mathbf{n}, \quad (25)$$

where $\tilde{\mathbf{z}}_t = [\tilde{z}_t(0), \ldots, \tilde{z}_t(N_c-1)]^T$ and the real and imaginary parts of $\{\tilde{z}_t(t); t=0\sim N_c-1\}$ are also an integer. Therefore, at the receiver, the soft decision variable can be obtained after the amplitude normalization and the modulo operation, similar to the conventional joint THP/pre-FDE.

The difference between the received signal vector $\mathbf{r}$ of the previously proposed joint THP/pre-FDE (see Eq. (12)) and the received signal vector $\mathbf{r}'$ of the proposed joint THP/pre-FDE using LLL-algorithm (see Eq. (25)) is the normalization coefficient. If $|B^L_{t,t}|$ near the rightmost position can be larger than $|B_{t,t}|$, the performance degradation can be mitigated. In the proposed scheme, the transmitter carries out the LLL-algorithm to compute $\mathbf{T}$, $\mathbf{B}^L$, and $\mathbf{Q}^L$. Although the application of the LLL-algorithm increases the computational complexity at the transmitter, the same simple signal detection can be done as the previously proposed joint THP/pre-FDE. Therefore, our proposed scheme is suitable for the downlink signal transmission.

IV. Computer Simulation

The proposed joint THP/pre-FDE using LLL-algorithm is evaluated by computer simulation. The simulation condition is summarized in Table 1. The propagation channel is assumed to be a frequency-selective block Rayleigh fading channel having an L=16-path uniform power delay profile. The number of FFT points is set as N_c=128 and we assume the GI length of N_g=16. Ideal channel estimation is assumed.

Table 1 Simulation condition

Data modulation		16QAM, 64QAM
No. of FFT points		N_c=128
No. of GI samples		N_g=16
Channel condition	Frequency-selective block Rayleigh	
	No. of paths	L=16
	Time delay	$\tau_l=l$ (l=0~L−1)
Channel estimation		Ideal

The cumulative distribution function (CDF) of $\{|B^L_{t,t}|; t=0\sim N_c-1\}$ is plotted in Fig. 4. For comparison, CDF of $\{|B_{t,t}|; t=0\sim N_c-1\}$ of the previously proposed joint THP/pre-FDE [8] is also plotted. It can be clearly seen from Fig. 4 that the probability that $|B^L_{t,t}|$ drops can be reduced. Also seen is that increasing δ decreases the probability that $|B^L_{t,t}|$ drops.

Figure 5 shows the average BER performance achievable with joint THP/pre-FDE using LLL-algorithm as a function of average transmit E_b/N_0(=$(1/N)E_s/N_0(1+N_g/N_c)$) for 16QAM (N=4) and 64QAM (N=6) data modulation. For comparison, the BER performance with previously proposed joint THP/pre-FDE that uses the dummy symbol insertion is also plotted (the number of dummy symbols is N_d). In the previously proposed joint THP/pre-FDE, when N_d=0, the BER performance significantly degrades since $|B_{t,t}|$ near the rightmost position drops. In [10], the dummy symbols of N_d=16 were used to avoid the BER degradation. However, this dummy symbol insertion results in the data rate loss and the E_b/N_0 loss. On the other hand, Fig. 5 shows that the use of LLL-algorithm for the joint THP/pre-FDE can avoid the BER degradation even without the dummy symbol insertion. By increasing the value of δ from 0, the BER performance of joint THP/pre-FDE with LLL-algorithm improves. However, the computational complexity increases [13]. Therefore, δ=0.5 can be used since the BER performance can be only slightly improved by increasing δ beyond 0.5.

V. Conclusion

In this paper, the application of LLL-algorithm to joint THP/pre-FDE was proposed to improve the BER performance without the insertion of the dummy symbols. This was confirmed by computer simulation.

Although the BER performance of joint THP/pre-FDE using LLL-algorithm is slightly worse than previously proposed joint THP/pre-FDE using dummy symbol insertion (N_d=16), the transmission data rate is higher. The throughput comparison is left for an important future study.

References

[1] F. Adachi, "Wireless past and future-evolving mobile communications systems," IEICE Trans. Fundamentals, Vol. E84-A, No. 1, pp. 55-60, Jan. 2001.

[2] J. G. Proakis, *Digital communications*, 2nd ed., McGraw-Hill, 1995.

[3] D. Falconer, S. L. Ariyavisitakul, A. Benyamin-Seeyar, and B. Edison, "Frequency-domain equalization for single-carrier broadband wireless systems," IEEE Commun., Mag., Vol. 40, No. 4, pp. 58-66, Apr. 2002.

[4] F. Adachi, D. Garg, S. Takaoka, and K. Takeda, "Broadband CDMA techniques," IEEE Wireless Commun., Mag., Vol. 12, No. 2, pp. 8-18, Apr. 2005.
[5] K. Takeda and F. Adachi, "Bit error rate analysis of DS-CDMA with joint frequency-domain equalization and antenna diversity reception," IEICE Trans. Commun., Vol. E87-B, No. 10, pp. 2991-3002, Oct. 2004.
[6] M. Tomlinson, "New automatic equalizer employing modulo arithmetic," Electronics Letters, Vol. 7, No. 5/6, pp. 138-139, Mar. 1971.
[7] H. Harashima and H. Miyakawa, "Matched-transmission technique for channels with intersymbol interference," IEEE Trans. Commun., Vol. 20, No. 4, pp. 774-780, Aug. 1972.
[8] K. Takeda, H. Tomeba, and F. Adachi, "BER performance analysis of joint Tomlinson-Harashima precoding and frequency-domain equalization," Proc. IEEE Wireless Communications and Networking Conference (WCNC), Hong Kong, Mar. 2007.
[9] K. Takeda, H. Tomeba, and F. Adachi, "Joint Tomlinson-Harashima precoding and frequency-domain equalization for broadband single-carrier transmission," IEICE Trans. Commun., Vol. E91-B, No. 1, pp. 258-266, Jan. 2008.
[10] K. Takeda, H. Tomeba, and F. Adachi, "BER performance of joint THP/pre-FDE," Proc. IEEE 67th Veh. Technol. Conf. (VTC), pp. 1016-1020, Singapore, May 2008.
[11] G. H. Golub, and C. F. Van Loan, *Matrix computations*, 2nd ed., The Johns Hopkins University Press, 1989.
[12] A. K. Lenstra, H. W. Lenstra, Jr., and L. Lovasz, "Factoring polynomials with rational coefficients," Math. Ann., Vol. 261, pp. 515-534, July 1982.
[13] C. P. Schnoor and M. Euchner, "Lattice basis reduction: improved practical alorithms and solving subset sum problems," Mathematical Programming, Vol. 66, pp. 181-191, July 1993.
[14] D. J. Lee, M. H. Park, and Y. S. Byun, "Near-maximum likelihood detection of MIMO systems using error detection scheme based lattice reduction," Proc. 12th Asia-pacific conference on communications (APCC), pp. 1-5, Busan, Korea, Aug. 2006.
[15] D. Wubben, R. Bohnke, V. Kuhn, and K. D. Kammeyer, "MMSE-based lattice-reduction for near-ML detection of MIMO systems," Proc. ITG workshop on smart antennas, pp. 106-113, Deutschland, Mar. 2004.
[16] R. Fisher, "The modulo-lattice channel: the key feature in precoding schemes," International Journal of Electronics and Communications, pp. 244-253, Jul. 2005.

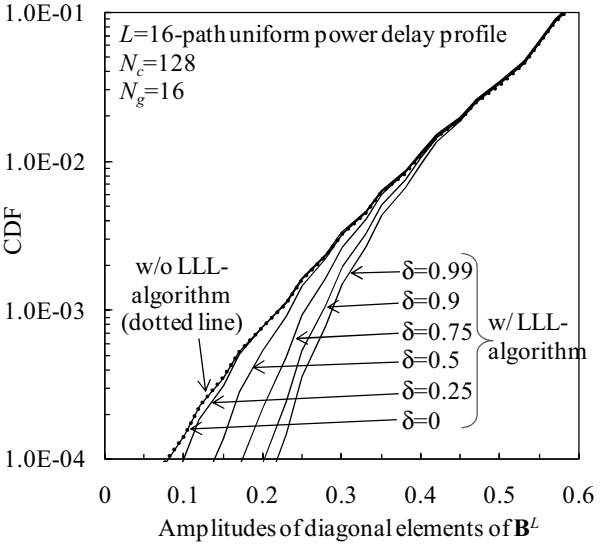

Fig. 4 CDF of $|B^{L}_{t,t}|$.

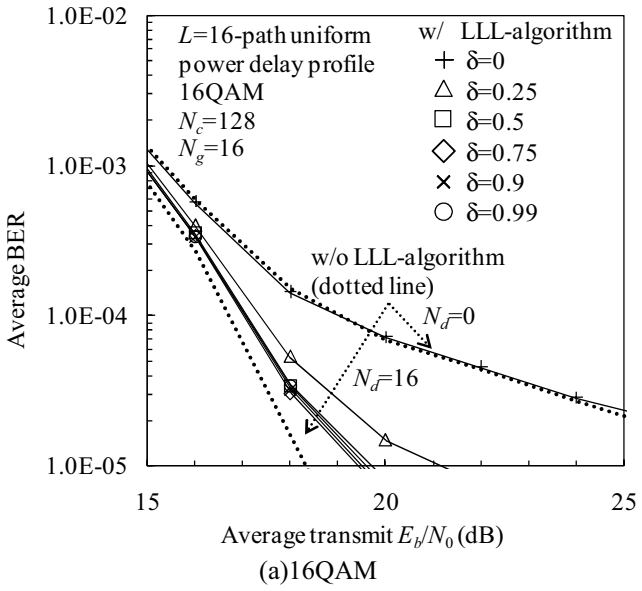

(a)16QAM

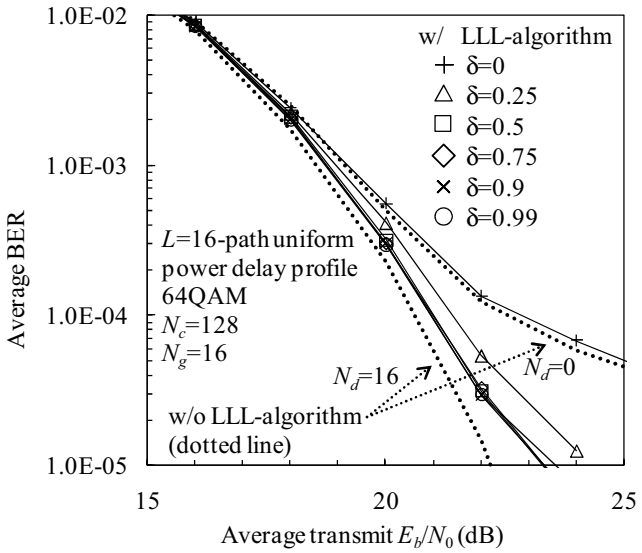

(b)64QAM

Fig. 5 BER performance.